Near-DC magnetic fields following a periodic presentation of long-duration tonebursts

C. Lammertmann and B. Lütkenhöner

Institute of Experimental Audiology, University of Münster, D-48129 Münster, Germany

1 Introduction

The auditory evoked potential (AEP) or magnetic field (AEF) elicited by a toneburst of sufficient duration can be decomposed into transient responses to stimulus on- and offset and a sustained response that lasts as long as the stimulus is present and generally appears as a baseline shift. It is well known that the sustained potential (SP) shows adaptation with prolonged stimulus duration [1]. Indications that also the sustained field (SF) tends to decrease with increasing latency are available as well [2]. Relatively little is known about slow magnetic field variations after stimulus offset. It is suggested at least by near DC-field measurements [3], [4] that this post-stimulatory decay is not instantaneous. Purpose of the present study was to answer the following questions. Does the SF show adaptation similiar to the SP? How does the field amplitude return to the prestimulus baseline after stimulus offset?

2 Methods

Tonebursts of 1 kHz and 10 s duration were presented at fixed 20 s intervals to the right ear of six right-handed subjects (4 f, 2 m, 21-37 y). AEFs were recorded contralateral to the side of stimulation, using a 37-channel first-order gradiometer system (Biomagnetic Technologies Inc.). 20 datasets were collected for each subject. Each measurement lasted 600 s, corresponding to 30 stimulus presentations. The averaged data (high-pass filtered, 0.03 Hz cut-off) were modelled using a single fixed dipole (1FD). The amplitudes derived for the dipole moment were fitted to exponentially decaying functions.

$$\text{Onset}: \qquad Q(t) = a + b\ \exp(-(t-1)/\tau_1) \qquad (1)$$

$$\text{Offset}: \qquad Q(t) = c\ \exp(-(t-0.75)/\tau_2) \qquad (2)$$

According to function (1) (fit range: 1–10 s after stimulus onset) the SF starts at an initial value $a + b$ (at time $t = 1\ s$) and declines with a time constant τ_1 to its asymptotic level a. In function (2) t specifies the time elapsed since stimulus offset. According to this function (fit range: 0.75–5 s) the near-DC field starts from the initial value c (at time $t = 0.75\ s$) and declines with a time constant τ_2.

3 Results

3.1 Exemplary data

The AEF has a clear transient on- and off-response as well as a less pronounced sustained response.

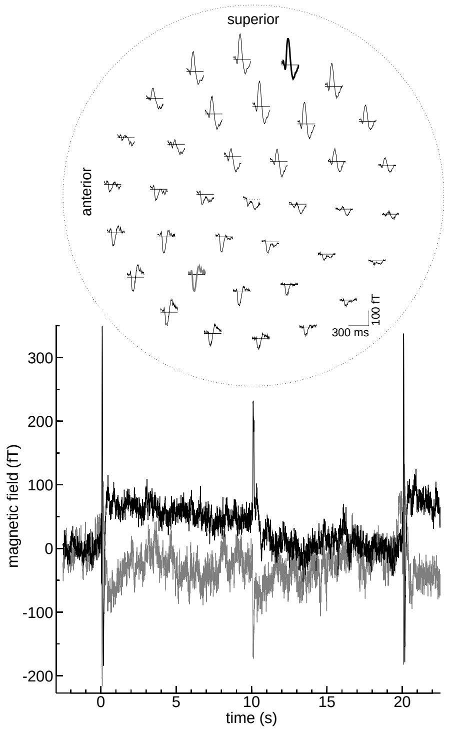

Figure 1: **Top:** *Sensor-layout display of the first 300 ms of the auditory evoked field (AEF) arising from a toneburst of 10 s duration.* **Bottom:** *Complete time course for two channels corresponding to the thick black and the thick grey curve in the upper part of the figure. On- and off- response appear as spikes near 0 s and 10 s. The noisy baseline shift in between represents the sustained field.*

In a sensor-layout display (Fig. 1, top) the two main components of the on-response, deflections N1m and P2m, can be easily identified. The dominant deflection in the curves is N1m, having a latency of about 90 ms in this subject. A deflection with opposite polarity, P2m, follows with a latency of about 170 ms. The curves exhibit a dipolar pattern, characterized by two field extrema with opposite polarity (deflection N1m has a positive value at the superior and a negative value at the inferior measurement location), and a zone with near-zero amplitudes in between. Fig. 1 (bottom) shows the complete time course for two channels corresponding to the thick black and thick grey curve in the upper part of the figure. On- and off-response appear as sharp spikes near 0 s and 10 s. The noisy baseline shift in between represents the sustained field.

3.2 Interindividual variability

The dipole moments derived from the four sessions were averaged. Fig. 2 shows the results for all six subjects. Again the transients appear as sharp spikes near 0 s and 10 s. The most prominent near DC-phenomenon, the SF, is evident in all six cases. This per-stimulatory response clearly exhibits adaptation with a certain interindividual variability. After stimulus offset, the time course of the estimated dipole moment returns to the baseline. A relatively poor signal-to-noise ratio may partially explain why the results obtained for subject A0050 were peculiar in several aspects. This subject will be excluded therefore from part of subsequent considerations.

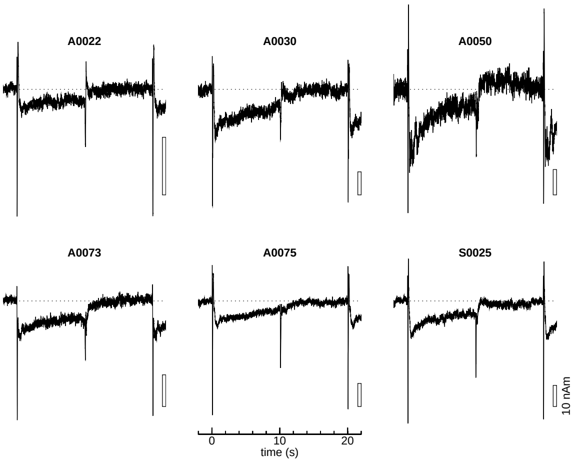

Figure 2: *Time courses of the dipole moments estimated for the six subjects. Each curve represents the average of four sessions.*

For a quantitative comparison of the time course of per-stimulatory adaptation and post-stimulatory decay, the exponential functions (1) and (2) were fitted to the data. A compilation of the results can be found in Table 1.

Table 1: *Parameters obtained by fitting the right-hand sides of equations (1) and (2) to the estimated dipole moments. In two cases (marked with an asterisk) the asymptotic value a had to be adjusted in advance to obtain reasonable time constants. The post-stimulatory decay could be analyzed only in four subjects.*

	per-stimulatory decay			post-stimulatory decay	
subject	a (nAm)	b/a	τ_1 (s)	c (nAm)	τ_2 (s)
A0022	-1.9	0.75	2.4	-0.6	1.8
A0030	-9.0^*	0.77	3.0	-3.9	1.9
A0050	$[-5.4]$	[2.83]	[2.8]	–	–
A0073	-5.4	0.74	3.0	-1.8	2.1
A0075	-4.0^*	1.18	4.1	-4.2	1.2
S0025	-5.1	1.53	4.0	–	–
median	-5.1	0.77	3.0	-2.9	1.9
mean	-5.1	0.99	3.3	-2.6	1.8
SD	2.6	0.35	0.75	1.7	0.38

Typical adaptation time constants (parameter τ_1) appear to be of the order 2.5-4 s (median 3 s), though a considerably longer time constant could not be excluded in subjects A0030 and A0075, where the limited signal-to-noise ratio hindered a clear distinction between an exponential and a linear decay. This problem was overcome by specifying the asymptotic level (parameter a) in advance, based on the mean dipole moment in the 500 ms interval immediately preceding stimulus offset. The value of parameter a exhibits a considerable variability, ranging from -1.9 nAm in subject A0022 to -9.0 nAm in subject A0030 (median -5.1 nAm). The parameter ratio b/a, which relates the amount of decay to the asymptotic value, turned out to be less variable. It varied between 0.74 in subject A0073 to 1.53 in subject S0025. Except for subjects S0025 and A0050, the asymptotic decay of the dipole moment after stimulus offset could be approximated by function (2). The amplitude c ranged from -0.6 nAm in subject A0022 to -4.2 nAm in subject A0075, and the time constant τ_2 from 1.2 s in subject A0075 to 2.1 s in subject A0073 (median 1.9 s).

3.3 Grand average of estimated dipole moment

Fig. 3 (calculated on the basis of all subjects except A0050) shows a grand average of normalized dipole moments. To ensure that all subjects contribute equally to the grand average, an amplitude normalization was carried out beforehand (division by the respective asymptotic value a given in Table 1).

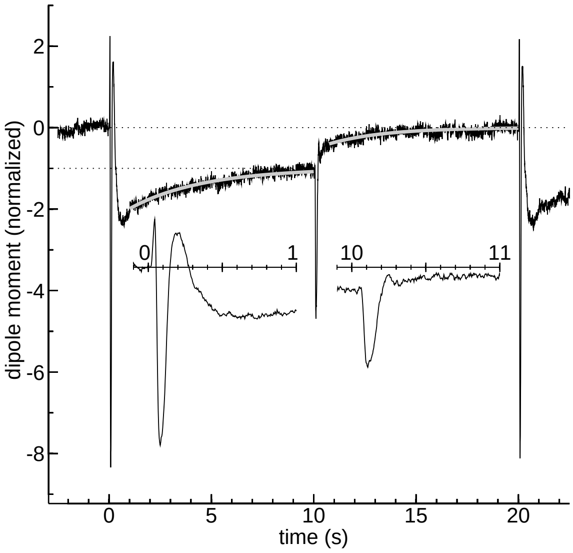

Figure 3: *Grand Average of normalized dipole moments from 5 subjects (subject A0050 excluded). The two insets show the time windows -0.1 s to 1 s (left) and 9.9 s to 11 s (right) in an enlarged scale.*

The signal-to-noise ratio of the grand average is evidently quite high, and especially the exponential decay after stimulus offset is much clearer than in the individual curves. Fitting the exponentially decaying functions (1) and (2) to the grand average (asymptotic level a of function (1) pre-defined as -1) resulted in the grey curves in Figu. 3. The good agreement with the grand-averaged experimental data suggests that the assumption of an exponential decay for both the SF and the near-DC field after stimulus offset is adequate. The fits for the grand-averaged data yielded an amplitude ratio b/a=0.99, and time constants τ_1=3.6 s and τ_2=2.7 s. The values obtained for the first two parameters agree well with the mean parameter values given in Table 1. The larger discrepancy for the latter parameter results from the fact, that subject S0025 (for which the asymptotic decay of the dipole moment after stimulus offset could not be approximated by function (2)) was used for the calculation of the grand average (omitting this subject resulted in τ_2=1.6 s).

3.4 Source locations

Fig. 4 shows the rough spatial relationship between the equivalent current dipole representing the SF, N1m, P2m and N1mOff in two orthogonal planes, the x-y plane (top) and the x-z plane (bottom). Like the dipoles representing the SF, dipoles for the other deflections were estimated using the 1FD model. The origin of the coordinate system was defined so that it corresponds to the equivalent current dipoles representing deflection N1m. The figure suggests that, in the group mean, the location (median of 4 sessions) of the SF generator and the N1m generator are basically the same. The generator of deflection P2m (which could be assessed only in subjects A0022, A0075, and S0025), was found about 1 cm anterior and about 0.7 cm inferior to the N1m generator.

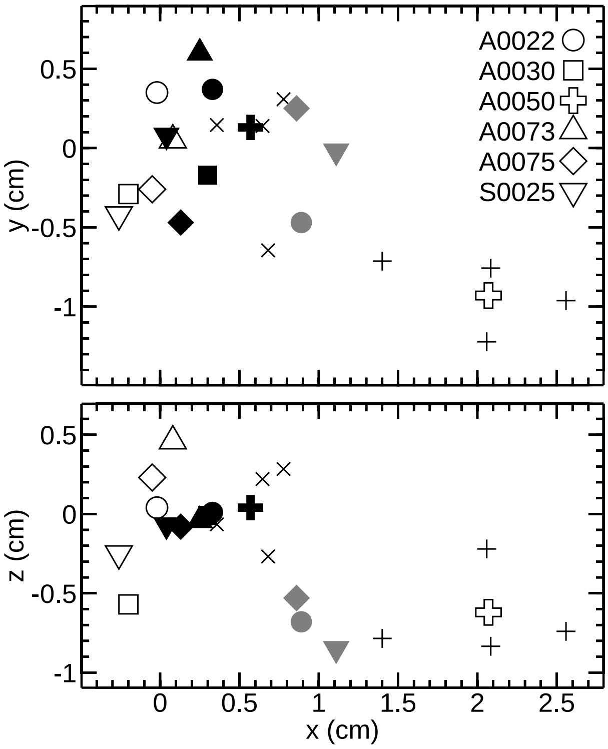

Figure 4: *Coordinates of estimated dipoles projected into two orthogonal planes (top: x-y plane; bottom: x-z plane). The origin of the coordinate system corresponds to the location estimated for deflection N1m. The unfilled, filled black, and filled grey symbols represent the coordinates estimated for the SF, N1mOff and P2m, respectively. All these symbols represent the median of four sessions. For one of the subjects (A0050, the subject with the worst signal-to-noise ratio) the locations derived from the four independent sessions are displayed as well (cross or symbol 'x').*

4 Discussion

This study demonstrated that magnetic fields in a frequency range below 0.1 Hz (near-DC) are accessible also to conventional measurement techniques, though special near-DC techniques (transformation of the near-DC fields to higher frequencies by moving the subject under the measurement system) are evidently required when going from near-DC to real DC. The SF shows adaptation similar to the SP. Its time course can be described quite well by an exponentially decaying function with a time constant of about 3.0 s. As a rule of thumb, the dipole moment at the beginning of the SF is about twice as high as the asymptotic value. After stimulus offset, the SF does not drop immediately to the baseline level, but is followed by a poststimulatory decay with a time constant of about 2.7 s.

Hari (1990) supposed that the SF may reflect activity of sustained-type cells during continuous input to the auditory cortex or summation of activity in transient cells. Possibly both explanations, sustained-type activity and summation of activity, contribute to the SF. Such a two-component model could explain at least some of the near-DC phenomena in the grand-average curve shown in Fig. 3. We hypothesize that one component, roughly follows the envelope of the stimulus, whereas the second component behaves like a leaky integrator. In such a model, which has been widely used for example in theoretical studies of action potential initiation, the effects of inputs sum linearly and decay exponentially with a certain time constant [6]. A suggestive hint of the hypothesized two-component model can be found at stimulus offset, where the near-DC field drops from the perstimulatory asymptotic level to a lower level, from which it decays exponentially to the baseline (representing the level of activity before stimulus onset). We attribute the almost instantaneous drop to the first component and the subsequent exponential decay to the second component. To explain the perstimulatory exponential decay, we assume, furthermore, that at least the input to the first component is subject to adaptation.

In magneto- or electroencephalographic investigations, near-DC fields are easily eliminated by high-pass filtering. This is, in fact, the common practice in almost all studies. However, when using functional imaging techniques like fMRI and PET, the activity actually measured represents a temporal integral, owing to the poor temporal resolution of these techniques. It is evident (compare Fig. 3) that integration of the response magnitudes over a few seconds or more increases the relative importance of near-DC phenomena considerably, whereas faster phenomena become less prominent. This consideration suggests that a better understanding of near-DC fields may be crucial for the understanding of the relationship between MEG and other functional imaging techniques like fMRI and PET.

Acknowledgements

This work was supported by the Deutsche Forschungsgesellschaft (grant Lu 342/4-2).

References

[1] T.W. Picton, D.L. Woods and G.B. Proulx, "Human auditory sustained potentials", *Electroencephalogr. Clin. Neurophysiol.* **45**, 186–210, 1978.

[2] C. Pantev, C. Eulitz, T. Elbert, M. Hoke, "The auditory evoked sustained field: origin and frequency dependence", *Electroencephalogr. Clin. Neurophysiol.* **90**, 82–90, 1994.

[3] G. Wübbeler et al., "Measurement of near-DC biomagnetic fields of the head using a horizontal modulation of the body position", in *Recent Advances in Biomagnetism*, Sendai: Tohoku University Press, 1999, pp. 369–372.

[4] G. Mackert et al., "Non-invasive long-term recordings of cortical ‘direct current‘ DC- activity in humans using magnetoencephalography", *Neurosci. Lett.* **273**, 159–162, 1999.

[5] R. Hari, "The neuromagnetic method in the study of the human auditory cortex", in *Auditory evoked magnetic fields and electric potentials*, Advances in Audiology, Vol. 6, Grandori, F., Hoke, M., and Romani, G., Ed. Basel: Karger, 1990, pp. 222–282.

[6] A. Holden, "Models of the stochastic activity of neurones", in *Lecture notes in Biomathematics 12*, New York: Springer, 1976.